Article

EULER–BERNOULLI BEAM THEORY:
FIRST-ORDER ANALYSIS, SECOND-ORDER ANALYSIS, STABILITY, AND VIBRATION ANALYSIS USING THE FINITE DIFFERENCE METHOD

Valentin Fogang

Abstract: This paper presents an approach to the Euler–Bernoulli beam theory (EBBT) using the finite difference method (FDM). The EBBT covers the case of small deflections, and shear deformations are not considered. The FDM is an approximate method for solving problems described with differential equations (or partial differential equations). The FDM does not involve solving differential equations; equations are formulated with values at selected points of the structure. The model developed in this paper consists of formulating partial differential equations with finite differences and introducing new points (additional points or imaginary points) at boundaries and positions of discontinuity (concentrated loads or moments, supports, hinges, springs, brutal change of stiffness, etc.). The introduction of additional points permits us to satisfy boundary conditions and continuity conditions. First-order analysis, second-order analysis, and vibration analysis of structures were conducted with this model. Efforts, displacements, stiffness matrices, buckling loads, and vibration frequencies were determined. Tapered beams were analyzed (e.g., element stiffness matrix, second-order analysis). Finally, a direct time integration method (DTIM) was presented. The FDM-based DTIM enabled the analysis of forced vibration of structures, the damping being considered. The efforts and displacements could be determined at any time.

Corresponding author: Valentin Fogang

                                  Civil Engineer

                                  C/o BUNS Sarl P.O Box 1130 Yaounde Cameroon

            E-mail: valentin.fogang@bunscameroun.com

            ORCID iD   https://orcid.org/0000-0003-1256-9862

1.   Introduction

The Euler–Bernoulli beam has been widely analyzed in the relevant literature. Several methods have been developed, e.g., the force method, the slope deflection method, and the direct stiffness method, etc. Anley et al. [1] considered a numerical difference approximation for solving two-dimensional Riesz space fractional convection-diffusion problem with source term over a finite domain. Kindelan et al. [2] presented a method to obtain optimal finite difference formulas which maximize their frequency range of validity. Both conventional and staggered equispaced stencils for first and second derivatives were considered. Torabi et al. [3] presented an exact closed-form solution for free vibration

analysis of Euler–Bernoulli conical and tapered beams carrying any desired number of attached masses. The concentrated masses were modeled by Dirac's delta functions. Katsikadelis [4] presented a direct time integration method for the solution of the equations of motion describing the dynamic response of structural linear and nonlinear multi-degree-of-freedom systems. The method applied also to equations with variable coefficients. Soltani et al. [5] applied the Finite Difference Method (FDM) to evaluate natural frequencies of non-prismatic beams, with different boundary conditions and resting on variable one or two parameter elastic foundations. Boreyri et al. [6] analyzed the free vibration of a new type of tapered beam, with exponentially varying thickness, resting on a linear foundation. The solution was based on a semi-analytical technique, the differential transform method. Mwabora et al. [7] considered numerical solutions for static and dynamic stability parameters of an axially loaded uniform beam resting on a simply supported foundations using Finite Difference Method where Central Difference Scheme was developed. The classical analysis of the Euler–Bernoulli beam consists of solving the governing equations (i.e., statics and material) that are expressed via means of differential equations, and considering the boundary and transition conditions. However, solving the differential equations may be difficult in the presence of an axial force (or external distributed axial forces), an elastic Winkler foundation, a Pasternak foundation, or damping (by vibration analysis). By the traditional analysis with FDM, points outside the beam were not considered. The boundary conditions were applied at the beam's ends and not the governing equations. The non-application of the governing equations at the beam's ends led to inaccurate results, making the FDM less interesting in comparison to other numerical methods such as the finite element method. In this paper, a model based on finite difference method was presented. This model consisted of formulating the differential equations (statics and material relation) with finite differences and introducing new points (additional points or imaginary points) at boundaries and at positions of discontinuity (concentrated loads or moments, supports, hinges, springs, and brutal change of stiffness, etc.). The introduction of additional points permitted us to satisfy boundary conditions and continuity conditions. First-order analysis, second-order analysis, and vibration analysis of structures were conducted with the model.

2.   Materials and methods

2.1   First-order analysis

The sign conventions adopted for loads, bending moments, shear forces, and displacements are illustrated in Figure 1.
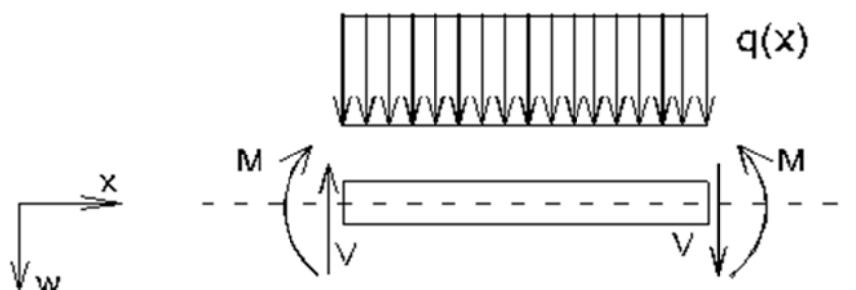
Figure 1.   Sign convention for loads, bending moments, shear forces, and displacements.

Specifically, M(x) is the bending moment in the section, V(x) is the shear force, w(x) is the deflection, and q(x) is the distributed load in the positive downward direction.

EULER–BERNOULLI BEAM THEORY USING THE FINITE DIFFERENCE METHOD

2.1.1 Uniform beam within segments

2.1.1.1 Statics

According to the Euler–Bernoulli beam theory (EBBT), the governing equation of a uniform beam loaded with q(x) is as follows:

$$EI\frac{d^4w(x)}{dx^4} + k(x)w(x) = q(x),$$

(1)

where EI is the flexural rigidity and $k(x)$ is the stiffness of the elastic Winkler foundation.

The bending moment, shear force, and slope $\varphi(x)$ are related to the deflection as follows:

$$M(x) = -EI\frac{d^2w(x)}{dx^2}$$

(2a)

$$V(x) = \frac{dM(x)}{dx} \rightarrow V(x) = -EI\frac{d^3w(x)}{dx^3}$$

(2b)

$$\varphi(x) = \frac{dw(x)}{dx}$$

(2c)

2.1.1.2 Fundamentals of FDM for a uniform beam

Figure 2 shows a segment of a beam having equidistant points with grid spacing h.
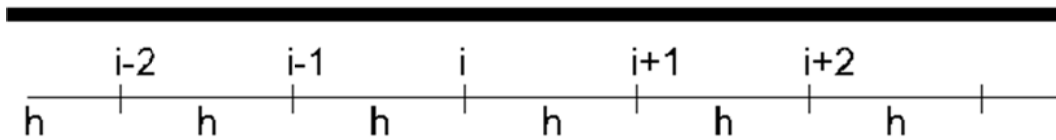
Figure 2. Beam with equidistant points.

The governing equation (Equation (1)) has a fourth order derivative, the deflection curve is consequently approximated around the point of interest i as a fourth degree polynomial.

Thus, the deflection curve can be described with the values of deflections at equidistant grid points:

$$w(x) = w_{i-2} \times f_{i-2}(x) + w_{i-1} \times f_{i-1}(x) + w_i \times f_i(x) + w_{i+1} \times f_{i+1}(x) + w_{i+2} \times f_{i+2}(x)$$

(3a)

The shape functions $f_j(x)$ (j = i-2; i-1; i; i+1; i+2) can be expressed using the Lagrange polynomials:

$$f_j(x) = \prod_{\substack{k=i-2 \\ k \neq j}}^{i+2} \frac{x - x_k}{x_j - x_k}$$

(3b)

Thus, a five-point stencil is used to write finite difference approximations to derivatives at grid points. Therefore, the derivatives at **i** are expressed with values of deflection at points i-2; i-1; i; i+1; i+2.

$$\left.\frac{d^4 w}{dx^4}\right|_i = \frac{w_{i-2} - 4w_{i-1} + 6w_i - 4w_{i+1} + w_{i+2}}{h^4} \tag{4a}$$

$$\left.\frac{d^3 w}{dx^3}\right|_i = \frac{-w_{i-2} + 2w_{i-1} - 2w_{i+1} + w_{i+2}}{2h^3} \tag{4b}$$

$$\left.\frac{d^2 w}{dx^2}\right|_i = \frac{-w_{i-2} + 16w_{i-1} - 30w_i + 16w_{i+1} - w_{i+2}}{12h^2} \tag{4c}$$

$$\left.\frac{dw}{dx}\right|_i = \frac{w_{i-2} - 8w_{i-1} + 8w_{i+1} - w_{i+2}}{12h} \tag{4d}$$

2.1.1.3 FDM Formulation of equations, efforts, and deformations

Let us consider a segment k of the beam having a flexural stiffness EI_k and equidistant grid points with spacing h_k. We introduce a reference flexural rigidity EI_r as follows

$$EI_k = \beta_k \times EI_r \tag{5}$$

We set

$$W(x) = EI_r \times w(x) \tag{5a}$$

Substituting Equations (4a), (5), and (5a) into Equation (1) yields

$$W_{i-2} - 4W_{i-1} + \left(6 + \frac{k_i h_k^4}{\beta_k EI_r}\right) W_i - 4W_{i+1} + W_{i+2} = \frac{1}{\beta_k} q_i h_k^4 \tag{6}$$

At point i, the bending moment, shear force, and slope are formulated with finite differences using Equations (2a–c), (4b–d), (5), and (5a).

$$M_i = \beta_k \frac{W_{i-2} - 16W_{i-1} + 30W_i - 16W_{i+1} + W_{i+2}}{12h_k^2} \tag{7a}$$

$$V_i = \beta_k \frac{W_{i-2} - 2W_{i-1} + 2W_{i+1} - W_{i+2}}{2h_k^3} \tag{7b}$$

$$EI_r \varphi_i = \frac{W_{i-2} - 8W_{i-1} + 8W_{i+1} - W_{i+2}}{12h_k} \tag{7c}$$

2.1.1.4 FDM Formulation of loadings

Let us determine here the FDM value q_i (Equation (6)) in the case of a varying distributed load q(x). Without considering the elastic Winkler foundation the distributed load q(x) is related to the shear force V(x) as follows:

$$q(x) = -\frac{dV(x)}{dx} \tag{8a}$$

Considering here a three-point stencil, the following FDM formulations of the first derivative can be made. The position i is considered as the left beam's end, an interior point on the beam, or the right beam's end, respectively:

$$\left.\frac{dV(x)}{dx}\right|_i = \frac{-3V_i + 4V_{i+1} - V_{i+2}}{2h} \tag{8b}$$

$$\left.\frac{dV(x)}{dx}\right|_i = \frac{-V_{i-1} + V_{i+1}}{2h} \tag{8c}$$

$$\left.\frac{dV(x)}{dx}\right|_i = \frac{V_{i-2} - 4V_{i-1} + 3V_i}{2h} \tag{8d}$$

The balance of vertical forces applied to a free body diagrams yields the following:

$$V_i - V_{i-1} = -\int_{i-1}^{i} q(x)dx \tag{8e}$$

$$V_{i+1} - V_i = -\int_{i}^{i+1} q(x)dx \tag{8f}$$

The combination of Equations (8a–f) yields the FDM value q_i for the position i being the left beam's end, an interior point on the beam, or the right beam's end.

$$q_i = \frac{1}{2h}\left[3\int_{i}^{i+1} q(x)dx - \int_{i+1}^{i+2} q(x)dx\right] \tag{8g}$$

$$q_i = \frac{1}{2h}\int_{i-1}^{i+1} q(x)dx \tag{8h}$$

$$q_i = \frac{1}{2h}\left[-\int_{i-2}^{i-1} q(x)dx + 3\int_{i-1}^{i} q(x)dx\right] \tag{8i}$$

The application of Equations (8g–8i) shows that in the case of a linearly distributed load, q_i is equal $q(x_i)$.

At point i, the stiffness of the elastic Winkler foundation k_i is calculated similarly to Equations (8g–8i).

2.1.1.5 Analysis at positions of discontinuity

Positions of discontinuity are positions of application of concentrated external loads (force or moment), supports, hinges, springs, abrupt change of cross section, and change of grid spacing.

2.1.1.5.1 Change of grid spacing

The discretization of the beam may lead to uniform-grid segments, but the grid spacings being different from one segment to another, as represented in Figure 3.

EULER–BERNOULLI BEAM THEORY USING THE FINITE DIFFERENCE METHOD
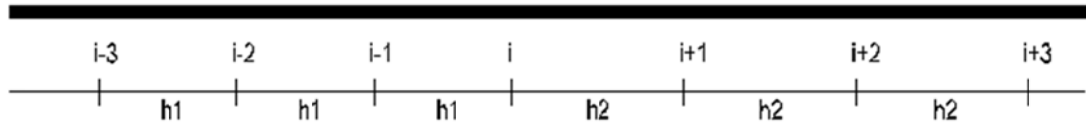
Figure 3.   Beam with different grid spacings.

The governing equation (Equation (6)), and the equations for the determination of the bending moment, shear force, and slope (Equations (7a-c)) at position i are formulated under consideration of different grid spacings h1 and h2.

2.1.1.5.2 Equations of continuity

Let us consider segments k and p of the beam having flexural stiffness EI_k and EI_p, and equidistant grid points with spacing h_k and h_p. Concentrated loads (force P and moment M^*) are applied at point i, as represented in Figure 4.
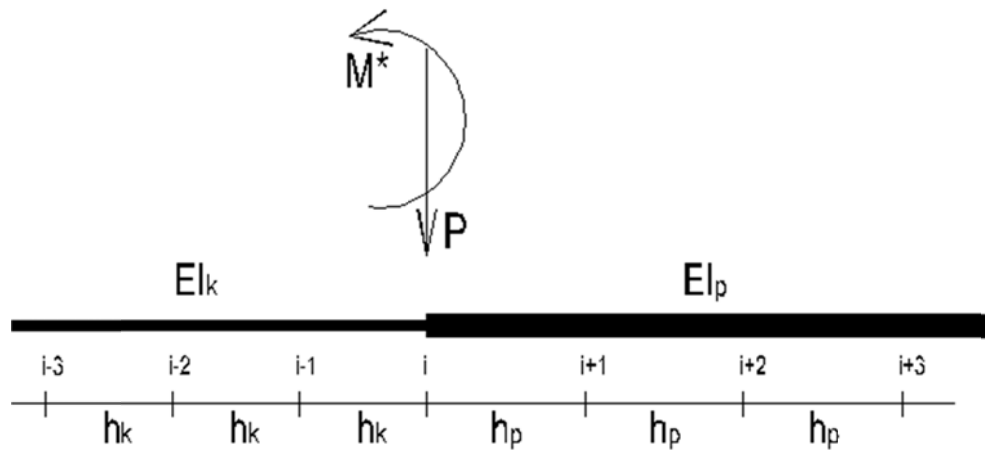
Figure 4. Beam with change in grid spacing and stiffness

The model developed in this paper consists of realizing an opening of the beam at point i and introducing additional points (fictive points **ia, ib, ic,** and **id**) in the opening, as represented in Figure 5a,b.

(5a)

(5b)
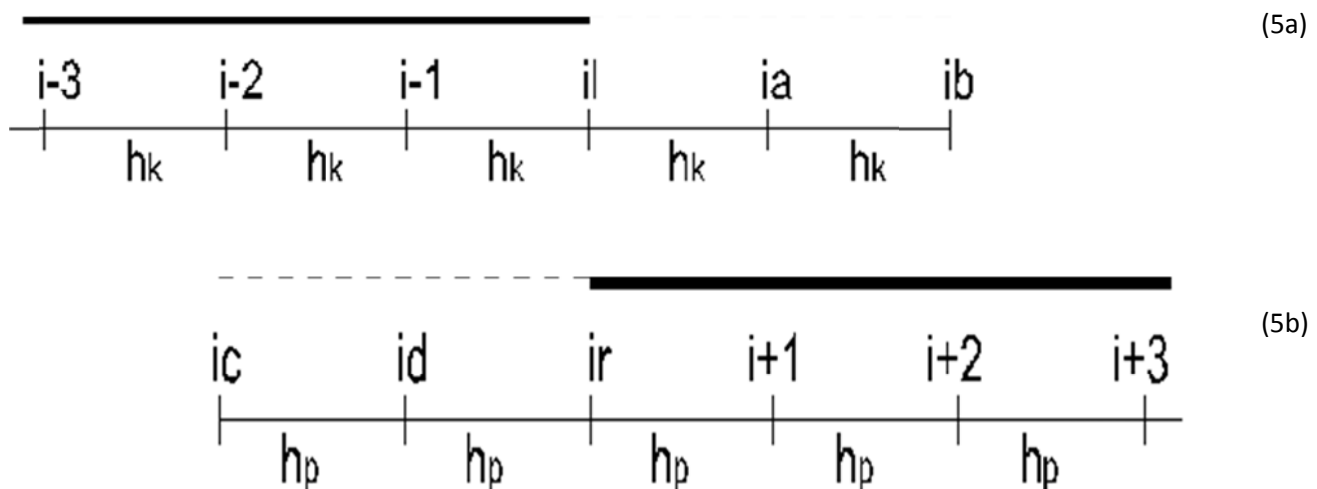
Figure 5a,b.   Opening of the beam and introduction of additional points on the left side (5a) and right side (5b).

EULER–BERNOULLI BEAM THEORY USING THE FINITE DIFFERENCE METHOD

The governing equation (Equation (6)) is applied at any point of the beam, i.e., i-2; i-1; il; ir; i+1; i+2, etc. Thus, the governing equations at positions il and ir yield:

$$W_{i-2} - 4W_{i-1} + \left(6 + \frac{k_{il}h_k^{\,4}}{\beta_k EI_r}\right)W_{il} - 4W_{ia} + W_{ib} = \frac{1}{\beta_k}q_{il}h_k^{\,4} \tag{9a}$$

$$W_{ic} - 4W_{id} + \left(6 + \frac{k_{ir}h_p^{\,4}}{\beta_p EI_r}\right)W_{ir} - 4W_{i+1} + W_{i+2} = \frac{1}{\beta_p}q_{ir}h_p^{\,4} \tag{9b}$$

The FDM formulations q_{il} and q_{ir} of distributed loading and k_{il} and k_{ir} of elastic Winkler foundation are calculated using Equations (8g-i).

The following continuity equations express the continuity of the deflection and slope (Equation (7c)), and the equilibrium of the bending moment (Equation (7a)) and shear force (Equation (7b)):

$$w_{il} = w_{ir} \rightarrow W_{il} = W_{ir} \tag{10a}$$

$$EI_r\varphi_{il} = EI_r\varphi_{ir} \rightarrow \frac{W_{i-2} - 8W_{i-1} + 8W_{ia} - W_{ib}}{12h_k} = \frac{W_{ic} - 8W_{id} + 8W_{i+1} - W_{i+2}}{12h_p} \tag{10b}$$

$$M_{il} - M_{ir} = M^* \rightarrow$$

$$\beta_k\frac{W_{i-2} - 16W_{i-1} + 30W_{il} - 16W_{ia} + W_{ib}}{12h_k^{\,2}} - \beta_p\frac{W_{ic} - 16W_{id} + 30W_{ir} - 16W_{i+1} + W_{i+2}}{12h_p^{\,2}} = M^* \tag{11}$$

$$V_{il} - V_{ir} = P \rightarrow \beta_k\frac{W_{i-2} - 2W_{i-1} + 2W_{ia} - W_{ib}}{2h_k^{\,3}} - \beta_p\frac{W_{ic} - 2W_{id} + 2W_{i+1} - W_{i+2}}{2h_p^{\,3}} = P \tag{12}$$

An adjustment of the continuity equations is made in case of a hinge (no continuity of the slope, $M_{il} = M_{ir} = 0$), a support ($W_{il} = W_{ir} = 0$, no equation (10d)), or a spring.

At the beam's ends, additional points are introduced (as shown in Figure 5a,b) and so governing equations are applied at the beam's ends, as well as the boundary conditions.

2.1.1.5.3   Non-uniform grid

The grid may be such that every node has a non-constant distance from another, as represented in Figure 6.
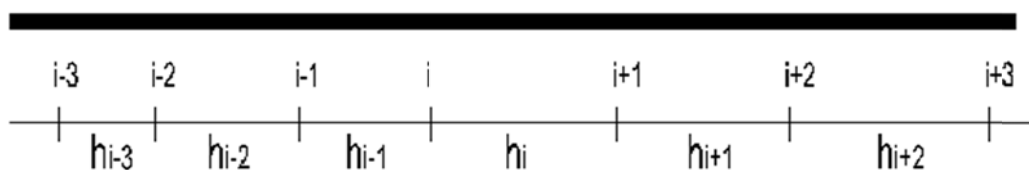
Figure 6.   Beam with a non-uniform grid.

Here, the Lagrange interpolation polynomial (Equation (3b)) is used for FDM formulation. The resulting equations are complicated, and consequently the non-uniform grid is not further analyzed in this paper. In fact, this case should not be analyzed as a discontinuity position.

2.1.2 First-order analysis of a tapered beam

2.1.2.1 Statics

Let us analyze here the case of a tapered beam, as shown in Figure 7.

Figure 7. Tapered beam.

An elastic Winkler foundation with stiffness k is considered. The varying flexural rigidity is $EI(x)$. The equations of static equilibrium and material relation are formulated as follows:

$$\frac{d^2 M(x)}{dx^2} - k(x)w(x) = -q(x) \tag{13a}$$

$$M(x) = -EI(x)\frac{d^2 w(x)}{dx^2} \tag{13b}$$

The slope is determined using Equation (2c), and the shear force using (2b).

2.1.2.2 FDM formulations of equations, efforts, and deformations

A uniform grid with spacing h_k is considered. Equations (13a-b) have a second order derivative; consequently, a three-point stencil is considered for the following derivatives (S(x) representing M(x) or w(x)):

$$\left.\frac{d^2 S(x)}{dx^2}\right|_i = \frac{S_{i-1} - 2S_i + S_{i+1}}{h_k^2} \tag{14a}$$

$$\left.\frac{dS(x)}{dx}\right|_i = \frac{-S_{i-1} + S_{i+1}}{2h_k} \tag{14b}$$

A reference flexural rigidity EI_r is introduced (Equations (5-5a)). Here the parameter β is defined at any position i. Considering Equations (5-5a) and (14a), the FDM formulations of Equations (13a,b) yield

$$\frac{M_{i-1} - 2M_i + M_{i+1}}{h_k^2} - k_i w_i = -q_i \rightarrow h_k^2 M_{i-1} - 2h_k^2 M_i + h_k^2 M_{i+1} - \frac{k_i h_k^4}{EI_r}W_i = -q_i h_k^4 \tag{15a}$$

$$M_i = -EI_i \frac{w_{i-1} - 2w_i + w_{i+1}}{h_k^2} \rightarrow h_k^2 M_i + \beta_i W_{i-1} - 2\beta_i W_i + \beta_i W_{i+1} = 0 \tag{15b}$$

EULER–BERNOULLI BEAM THEORY USING THE FINITE DIFFERENCE METHOD

At any point on the grid, Equations (15a-b) are applied. The unknowns are the deflection and bending moment. The application of Equations (2b), (2c), and (14b) yields the shear force and slope:

$$V_i = \left.\frac{dM(x)}{dx}\right|_i = \frac{-M_{i-1} + M_{i+1}}{2h_k} \tag{15c}$$

$$\varphi_i = \left.\frac{dw(x)}{dx}\right|_i = \frac{-w_{i-1} + w_{i+1}}{2h_k} \tag{15d}$$

2.1.2.3 Analysis of a tapered beam at positions of discontinuity

Concentrated loads (force P and moment M^*) are applied at point i (see Figure 4). A change in grid spacing is also assumed at this position. As described in section 2.1.1.5, an opening of the beam at point i introduced additional points (points **ia** and **id**) in the opening, as represented in Figure 8a,b.

(8a)

(8b)
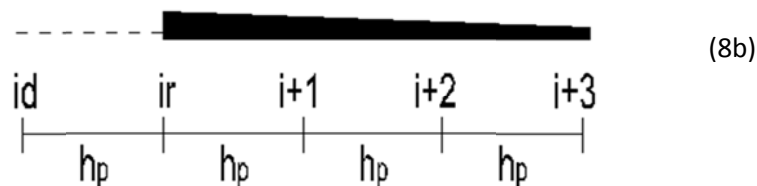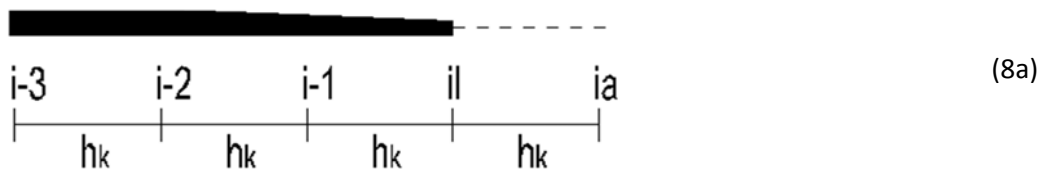
Figure 8a,b.   Opening of the beam and introduction of additional points at the left side (8a) and right side (8b).

The additional points are ia and id, and the unknowns are w_{ia}, M_{ia}, w_{id}, and M_{id}.

The continuity equations express the continuity of the deflection and slope (Equation (15d)), and the equilibrium of the bending moment and shear force (Equation (15c)) as follows:

$$w_{il} = w_{ir} \rightarrow W_{il} = W_{ir} \tag{16a}$$

$$EI_r \varphi_{il} = EI_r \varphi_{ir} \rightarrow \frac{-W_{i-1} + W_{ia}}{2h_k} = \frac{-W_{id} + W_{i+1}}{2h_p} \tag{16b}$$

$$M_{il} - M_{ir} = M^* \tag{16c}$$

$$V_{il} - V_{ir} = P \rightarrow \frac{-M_{i-1} + M_{ia}}{2h_k} - \frac{-M_{id} + M_{i+1}}{2h_p} = P \tag{16d}$$

At a point i with a hinge the slopes are not more equal, and the moments M_{il} and M_{ir} are zero.

EULER–BERNOULLI BEAM THEORY USING THE FINITE DIFFERENCE METHOD

2.1.3   First-order element stiffness matrix of a tapered beam

2.1.3.1   4×4 element stiffness matrix

The sign conventions for bending moments, shear forces, displacements, and slope adopted for use in determining the element stiffness matrix in local coordinates is illustrated in Figure 9.

Figure 9. Sign conventions for moments, shear forces, displacements, and slopes for stiffness matrix.

Let us define following vectors:

$$\overrightarrow{S_{red}} = \left[V_i ; M_i ; V_k ; M_k \right]^T \tag{17a}$$

$$\overrightarrow{V_{red}} = \left[w_i ; \varphi_i ; w_k ; \varphi_k \right]^T \tag{17b}$$

The 4×4 element stiffness matrix in local coordinates of the tapered beam is denoted by K_{44}.

The vectors above are related together with the element stiffness matrix K_{44} as follows:

$$\overrightarrow{S_{red}} = K_{44} \times \overrightarrow{V_{red}} \tag{18}$$

Let us divide the beam in n parts of equal length h (l =nh) as shown in Figure 10.
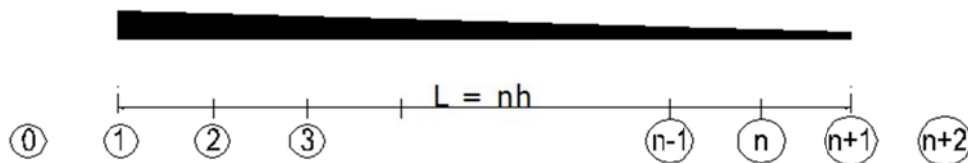
Figure 10. Finite difference method (FDM) discretization for 4x4 element stiffness matrix.

Equations (15a) with q_i =0 and (15b) are applied at any point on the grid (positions 1; 2; …n+1 of Figure 10).

Considering the sign conventions adopted for bending moments and shear forces in general (see Figure 1) and for bending moments and shear forces in the element stiffness matrix (see Figure 9), we can set following static compatibility boundary conditions in combination with Equations (2b) and (14b):

$$V_i = -V_1 = -\frac{dM(x)}{dx}\bigg|_1 = -\frac{M_2 - M_0}{2h} \rightarrow 2hV_i + M_2 - M_0 = 0 \tag{19a}$$

$$M_i = M_1 \rightarrow M_i - M_1 = 0 \tag{19b}$$

EULER–BERNOULLI BEAM THEORY USING THE FINITE DIFFERENCE METHOD

$$V_k = V_{n+1} = \frac{dM(x)}{dx}\bigg|_{n+1} = \frac{M_{n+2} - M_n}{2h} \rightarrow 2hV_k - M_{n+2} + M_n = 0 \tag{19c}$$

$$M_k = -M_{n+1} \rightarrow M_k + M_{n+1} = 0 \tag{19d}$$

Considering the sign conventions adopted for the displacements and slope in general (see Figure 1) and for displacements and slope in the element stiffness matrix (see Figure 9), we can set following geometric compatibility boundary conditions in combination with Equations (2c) and (14b):

$$w_1 = w_i \rightarrow W_1 = EI_r \times w_i \tag{20a}$$

$$\varphi_1 = \frac{dw(x)}{dx}\bigg|_1 = \frac{-w_0 + w_2}{2h} = \varphi_i \rightarrow \frac{-W_0 + W_2}{2h} = EI_r \times \varphi_i \tag{20b}$$

$$w_{n+1} = w_k \rightarrow W_{n+1} = EI_r \times w_k \tag{20c}$$

$$\varphi_{n+1} = \frac{dw(x)}{dx}\bigg|_{n+1} = \frac{-w_n + w_{n+2}}{2h} = \varphi_k \rightarrow \frac{-W_n + W_{n+2}}{2h} = EI_r \times \varphi_k \tag{20d}$$

The number of equations is $2(n+1) + 4 + 4 = \textbf{2n + 10}$. The number of unknowns is $2(n+3) + 4 = \textbf{2n + 10}$, especially $2(n+3)$ unknowns (M; W) at points on the beam and additional points at beam's ends, and 4 efforts at beam's ends (V_i; M_i; V_k; M_k). Let us define following vector

$$\vec{S}_1 = \left[M_0; W_0; M_1; W_1 \ldots M_{n+2}; W_{n+2} \right]^T \tag{21}$$

The combination of Equations (15a,b) applied at any point on the grid, Equations (19a–d), and Equations (20a–d) can be expressed with matrix notation as follows, the geometric compatibility boundary conditions (Equations (20a–d)) being at the bottom.

$$T \times \begin{bmatrix} \vec{S}_1 \\ \vec{S}_{red} \end{bmatrix} = \begin{bmatrix} \vec{0} \\ EI_r \times \vec{V}_{red} \end{bmatrix} \rightarrow \begin{bmatrix} \vec{S}_1 \\ \vec{S}_{red} \end{bmatrix} = T^{-1} \times \begin{bmatrix} \vec{0} \\ EI_r \times \vec{V}_{red} \end{bmatrix} \tag{22}$$

The matrix **T** has 2n+10 rows and 2n+10 columns. The zero vector above has 2n+6 rows.

$$T^{-1} = \begin{bmatrix} T_{aa} & T_{ab} \\ T_{ba} & T_{bb} \end{bmatrix} \tag{23}$$

The matrix T_{aa} has 2n+6 rows and 2n+6 columns, the matrix T_{ab} has 2n+6 rows and 4 columns, the matrix T_{ba} has 4 rows and 2n+6 columns, and the matrix T_{bb} has 4 rows and 4 columns.

The combination of Equations (18), (22), and (23) yields the element stiffness matrix of the beam.

$$K_{44} = EI_r \times T_{bb} \tag{24a}$$

A general matrix formulation of K_{44} is as follows:

$$K_{44} = EI_r \times \begin{bmatrix} 0 & I \end{bmatrix} \times T^{-1} \times \begin{bmatrix} 0^T \\ I \end{bmatrix} \tag{24b}$$

In Equation (24b), 0 is a zero matrix with four rows and 2n+6 columns, I is the 4×4 identity matrix.

2.1.3.2   3×3 element stiffness matrix

Assuming the presence of a hinge at the right end, the sign convention for bending moments, shear forces, displacements, and slope is illustrated in Figure 11.

Figure 11. Sign conventions for moments, shear forces, displacements, and slope for stiffness matrix.

The 3×3 element stiffness matrix in local coordinates of the tapered beam is denoted by K_{33}.

The vectors of Equations (17a), (17b), and (18) become

$$\overrightarrow{S_{red}} = \begin{bmatrix} V_i; M_i; V_k \end{bmatrix}^T \tag{25a}$$

$$\overrightarrow{V_{red}} = \begin{bmatrix} w_i; \varphi_i; w_k \end{bmatrix}^T \tag{25b}$$

$$\overrightarrow{S_{red}} = K_{33} \times \overrightarrow{V_{red}} \tag{25c}$$

The matrix K_{33} can be formulated with the values of the matrix K_{44} (see Equations (24a–b)).

$$K_{44} = \begin{bmatrix} K_{aa} & K_{ab} \\ K_{ba} & K_{bb} \end{bmatrix} \tag{26}$$

K_{44} has 4 rows and 4 columns. The matrix K_{aa} has 3 rows and 3 columns, the matrix K_{ab} has 3 rows and 1 column, the matrix K_{ba} has 1 row and 3 columns, and the matrix K_{bb} has 1 row and 1 column (a single value).

The combination of Equation (18) with the presence of a hinge at position k ($M_k = 0$), and Equation (25c) yields the matrix K_{33} as follows:

$$K_{33} = K_{aa} - K_{ab} \times \frac{1}{K_{bb}} \times K_{ba} \tag{27}$$

EULER–BERNOULLI BEAM THEORY USING THE FINITE DIFFERENCE METHOD

2.1.4   First-order element stiffness matrix of a uniform beam

The beam is divided in n parts of equal length h (l =nh) as shown in Figure 12.
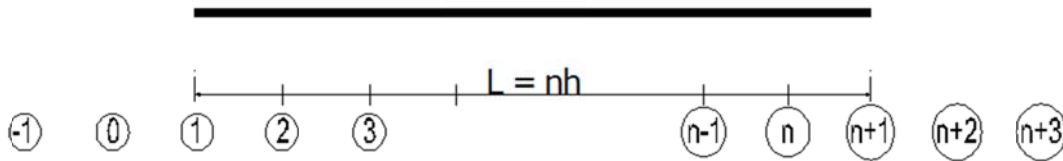
Figure 12. FDM discretization for 4x4 element stiffness matrix.

Equation (6) with $q_i = 0$ is applied at any point on the grid (positions 1; 2; …n+1 of Figure 12).

The static compatibility boundary conditions (Equations (19a–d)) become

$$V_i = -V_1 = -\beta_k \times \frac{W_{-1} - 2W_0 + 2W_2 - W_3}{2h^3} \rightarrow \frac{2h^3}{\beta_k} V_i + W_{-1} - 2W_0 + 2W_2 - W_3 = 0 \qquad (28a)$$

$$M_i = M_1 = \beta_k \times \frac{W_{-1} - 16W_0 + 30W_1 - 16W_2 + W_3}{12h^2}$$

$$\rightarrow \frac{12h^2}{\beta_k} M_i - W_{-1} + 16W_0 - 30W_1 + 16W_2 - W_3 = 0 \qquad (28b)$$

$$V_k = V_{n+1} = \beta_k \times \frac{W_{n-1} - 2W_n + 2W_{n+2} - W_{n+3}}{2h^3}$$

$$\rightarrow \frac{2h^3}{\beta_k} V_k - W_{n-1} + 2W_n - 2W_{n+2} + W_{n+3} = 0 \qquad (28c)$$

$$M_k = -M_{n+1} = -\beta_k \times \frac{W_{n-1} - 16W_n + 30W_{n+1} - 16W_{n+2} + W_{n+3}}{12h^2}$$

$$\rightarrow \frac{12h^2}{\beta_k} M_k + W_{n-1} - 16W_n + 30W_{n+1} - 16W_{n+2} + W_{n+3} = 0 \qquad (28d)$$

The geometric compatibility boundary conditions (Equations (20b,d)) become

$$\varphi_1 = \frac{dw(x)}{dx}\bigg|_1 = \frac{w_{-1} - 8w_0 + 8w_2 - w_3}{12h} = \varphi_i$$

$$\rightarrow \frac{W_{-1} - 8W_0 + 8W_2 - W_3}{12h} = EI_r \times \varphi_i \qquad (29a)$$

$$\varphi_{n+1} = \frac{dw(x)}{dx}\bigg|_{n+1} = \frac{w_{n-1} - 8w_n + 8w_{n+2} - w_{n+3}}{12h} = \varphi_k$$

$$\rightarrow \frac{W_{n-1} - 8W_n + 8W_{n+2} - W_{n+3}}{12h} = EI_r \times \varphi_k \qquad (29b)$$

Equations (20a) and (20c) stay unchanged.

Thus, the number of equations is n+**9**. The number of unknowns is n+5 + 4 = **n + 9**, especially n+5 unknowns W (at points on the beam and additional points at beam's ends) and 4 efforts at beam's ends (V_i; M_i; V_k; M_k).

The vector $\vec{S}_1$ becomes,

$$\vec{S}_1 = \left[W_{-1}; W_0; W_1 .... W_{n+1}; W_{n+2}; W_{n+3} \right]^T \tag{29c}$$

The use of Equations (22) to (24b) yields the element stiffness matrix of the uniform beam.

2.2   Second-order analysis

The equation of static equilibrium can be expressed as follows:

$$\frac{d^2 M(x)}{dx^2} + \frac{d}{dx}\left(N(x)\frac{dw(x)}{dx} \right) - k(x)w(x) = -q(x) \tag{30}$$

The axial force (positive in tension) is denoted by $N(x)$, and the stiffness of the elastic Winkler foundation by $k(x)$. Let us also consider an external distributed axial load $n(x)$ positive along the + x axis

$$n(x) = -\frac{dN(x)}{dx} \tag{31}$$

Combining Equations (30) and (31) yields

$$\frac{d^2 M(x)}{dx^2} + N(x)\frac{d^2 w(x)}{dx^2} - n(x)\frac{dw(x)}{dx} - k(x)w(x) = -q(x) \tag{32}$$

2.2.1 Constant stiffness EI within segments of the beam

A beam with constant stiffness in segments was considered. Substituting Equation (2a) into Equation (32) yields

$$-EI\frac{d^4 w(x)}{dx^4} + N(x)\frac{d^2 w(x)}{dx^2} - n(x)\frac{dw(x)}{dx} - k(x)w(x) = -q(x) \tag{33}$$

Substituting Equations (4a), (4c), (4d), (5), and (5a) into Equation (33) yields the following governing equation,

$$(\beta_i + \frac{N_i h^2}{12EI_r} + \frac{n_i h^3}{12EI_r})W_{i-2} + (-4\beta_i - \frac{4N_i h^2}{3EI_r} - \frac{2n_i h^3}{3EI_r})W_{i-1} + (6\beta_i + \frac{5N_i h^2}{2EI_r} + \frac{k_i h^4}{EI_r})W_i$$

$$+(-4\beta_i - \frac{4N_i h^2}{3EI_r} + \frac{2n_i h^3}{3EI_r})W_{i+1} + (\beta_i + \frac{N_i h^2}{12EI_r} - \frac{n_i h^3}{12EI_r})W_{i+2} = q_i h^4 \tag{34}$$

Equation (34) is applied at any point on the grid with spacing h. At point i, the external distributed axial load n_i is calculated similarly to Equations (8g–i). The transverse force $T(x)$ is related to the shear force $V(x)$ as follows:

$$T(x) = V(x) + N(x)\frac{dw(x)}{dx} \tag{35}$$

Substituting Equations (2b), (4b), (4d), (5), and (5a) into (35) yields the FDM formulation of the transverse force

$$T_i = -EI_i \left.\frac{d^3 w}{dx^3}\right|_i + N_i \left.\frac{dw}{dx}\right|_i \tag{36}$$

$$\rightarrow 2h^3 T_i = (\beta_i + \frac{Nh^2}{6EI_r})W_{i-2} + (-2\beta_i - \frac{4Nh^2}{3EI_r})W_{i-1} + (2\beta_i + \frac{4Nh^2}{3EI_r})W_{i+1} + (-\beta_i - \frac{Nh^2}{6EI_r})W_{i+2}$$

The bending moment and the slope are formulated using Equations (7a) and (7c), respectively.

The analysis at positions of discontinuity is conducted similarly to that of the first-order analysis; however the shear force is replaced by the transverse force.

2.2.2   Second-order analysis of a tapered beam

Applying Equations (5), (5a), (14a-b), in Equation (32) yields The FDM formulation of Equation (32) as follows:

$$h^2 M_{i-1} - 2h^2 M_i + h^2 M_{i+1} + \left(\frac{N_i h^2}{EI_r} + \frac{n_i h^3}{2EI_r} \right)W_{i-1} - \left(\frac{2N_i h^2}{EI_r} + \frac{k_i h^4}{EI_r} \right)W_i$$

$$+ \left(\frac{N_i h^2}{EI_r} - \frac{n_i h^3}{2EI_r} \right)W_{i+1} = -q_i h^4 \tag{37}$$

Equations (37) and (15b) are applied at any point on the grid.

The combination of Equations (35), (15c), and (15d) yields the FDM formulation of the transverse force

$$2h^3 T_i = h^2 M_{i+1} - h^2 M_{i-1} + \frac{N_i h^2}{EI_r}\left(W_{i+1} - W_{i-1}\right) \tag{38}$$

The slope is calculated similarly to Equation (15d).

The analysis at positions of discontinuity is conducted similarly to that of the first-order analysis; however the shear force is replaced by the transverse force.

2.2.3   Second-order element stiffness matrix of a tapered beam

The sign conventions for bending moments, transversal forces, displacements, and slopes adopted for use in determining the element stiffness matrix in local coordinates is illustrated in Figure 13.

Figure 13. Sign conventions for moments, transversal forces, displacements, and slopes for stiffness matrix.

The FDM discretization is the same as Figure 10. Equations (17a) becomes,

$$\overrightarrow{S_{red}} = \left[T_i \, ; M_i \, ; T_k \, ; M_k \right]^T \tag{39}$$

Equations (37) and (15b) are applied at any point on the grid (the distributed load q_i being zero).

The static compatibility boundary conditions are expressed similarly to Equations (19a–d); however in Equations (19a) and (19c), the shear forces are replaced by the transverse forces (Equation (38)). The analysis continues similar to the first-order element stiffness matrix (Equations (20a–24b)).

2.3   Vibration analysis of the beam

2.3.1   Free vibration analysis

Our focus here is to determine the eigenfrequencies of the beams. Damping is not considered. A second-order analysis is conducted; the first-order analysis can easily be deduced.

2.3.1.1   Beam with constant stiffness EI within segments

The governing equation is as follows:

$$EI \frac{\partial^4 w^*(x,t)}{\partial x^4} - N(x) \frac{\partial^2 w^*(x,t)}{\partial x^2} + n(x) \frac{\partial w^*(x,t)}{\partial x} + k(x) w^*(x,t) + \rho A \frac{\partial^2 w^*(x,t)}{\partial t^2} = 0 \tag{40}$$

where ρ is the beam's mass per unit volume, A is the cross-sectional area, N(x) is the axial force (positive in tension), n(x) is the external distributed axial load positive along + x axis, and k is the stiffness of the elastic Winkler foundation. A harmonic vibration being assumed, w^*(x,t) can be expressed as follows:

$$w^*(x,t) = w(x) \times \sin(\omega t + \theta) \tag{41}$$

Here, ω is the circular frequency of the beam. Substituting Equation (41) into Equation (40) yields

$$EI \frac{d^4 w(x)}{dx^4} - N(x) \frac{d^2 w(x)}{dx^2} + n(x) \frac{dw(x)}{dx} + k(x) w(x) - \rho A \omega^2 w(x) = 0 \tag{42}$$

A uniform grid with spacing h_k is assumed in the segment k.

Substituting Equations (4a), (4c-d), (5), and (5a) into Equation (42) yields the following governing equation:

$$(\beta_k + \frac{N_i h_k^2}{12 EI_r} + \frac{n_i h_k^3}{12 EI_r}) W_{i-2} + (-4\beta_k - \frac{4 N_i h_k^2}{3 EI_r} - \frac{2 n_i h_k^3}{3 EI_r}) W_{i-1} + (6\beta_k + \frac{5 N_i h_k^2}{2 EI_r} + \frac{k_i h_k^4}{EI_r} - \frac{\rho A_k \omega^2 h_k^4}{EI_r}) W_i$$

$$+ (-4\beta_k - \frac{4 N_i h_k^2}{3 EI_r} + \frac{2 n_i h_k^3}{3 EI_r}) W_{i+1} + (\beta_k + \frac{N_i h_k^2}{12 EI_r} - \frac{n_i h_k^3}{12 EI_r}) W_{i+2} = 0 \tag{43a}$$

Equation (43a) is applied at any point on the grid. The slope, the bending moment, and the transverse force are determined using Equations (7c), (7a), and (36), respectively.

Let us define a reference length l_r, a reference cross-sectional area A_r and the vibration coefficient λ as follows

$$h_k = \beta_{lk} l_r \qquad (43b)$$

$$A_k = \beta_{Ak} A_r \qquad (43c) \qquad\qquad \omega = \lambda \times \sqrt{\frac{EI_r}{\rho A_r l_r^4}} \rightarrow \frac{\rho A_k \omega^2 h_k^4}{EI_r} = \beta_{Ak} \beta_{lk}^4 \lambda^2 \quad (43d)$$

A change in grid spacing can be modeled by means of the reference length and the parameters β_{lk}.

For the special case of a uniform beam without an axial force or a Winkler foundation, Equation (43a) becomes

$$W_{i-2} - 4W_{i-1} + (6 - \beta_{lk}^4 \lambda^2)W_i - 4W_{i+1} + W_{i+2} = 0 \qquad\qquad (43e)$$

Effect of a concentrated mass, or a spring

We analyzed the dynamic behavior of a beam carrying a concentrated mass or having a spring, as represented in Figure 14.

Figure 14.   Vibration of beam having a concentrated mass and a spring.

The stiffness of the spring is K_p, and the concentrated mass is M_p.

$$K_p = k_p \times EI_r / l_r^3 \qquad\qquad (44a)$$

$$M_p = m_p \times \rho A_r l_r \qquad\qquad (44b)$$

The continuity equations for deflection, slope, and bending moment are defined in Equations (10a), (10b), and (11), respectively. Equation (11) is applied with $M^* = 0$. The reference length of the beam is l_r ((Equation (43b)).

Applying Equations (43d) and (44a-b), the balance of vertical forces in case of a concentrated mass or a spring yields

$$T_{il} - T_{ir} - \frac{M_p \omega^2}{EI_r} W_{il} = 0 \rightarrow T_{il} - T_{ir} - \frac{m_p}{l_r^3} \lambda^2 W_{il} = 0 \qquad\qquad (45a)$$

$$T_{il} - T_{ir} + \frac{K_p}{EI_r} W_{il} = 0 \rightarrow T_{il} - T_{ir} + \frac{k_p}{l_r^3} W_{il} = 0 \qquad\qquad (45b)$$

The transverse forces T_{il} and T_{ir} are calculated using Equation (36).

Effect of a spring–mass system: We analyzed the dynamic behavior of a beam carrying a spring–mass system, as represented in Figure 15. The deflection of the mass is denoted by W_{iM}.
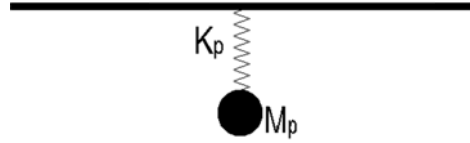
Figure 15.   Vibration of a beam carrying a spring–mass system.

Applying Equations (43d) and (44a-b), the balance of vertical forces yields

$$T_{il} - T_{ir} - \frac{M_p \omega^2}{EI_r} W_{iM} = 0 \rightarrow T_{il} - T_{ir} - \frac{m_p}{l_r^3} \lambda^2 W_{iM} = 0 \tag{45c}$$

$$\frac{M_p \omega^2}{EI_r} W_{iM} = \frac{K_p}{EI_r} \times (W_{iM} - W_{ir}) \rightarrow m_p \lambda^2 W_{iM} = k_p (W_{iM} - W_{ir}) \tag{45d}$$

2.3.1.2 Tapered beam

The governing equations are as follows:

$$\frac{\partial^2 M^*(x,t)}{\partial x^2} + N(x)\frac{\partial^2 w^*(x,t)}{\partial x^2} - n(x)\frac{\partial w^*(x,t)}{\partial x} - k(x)w^*(x,t) - \rho A(x)\frac{\partial^2 w^*(x,t)}{\partial t^2} = 0 \tag{46a}$$

$$M^*(x,t) = -EI(x)\frac{\partial^2 w^*(x,t)}{\partial x^2} \tag{46b}$$

A harmonic vibration being assumed, $M^*(x,t)$ can be expressed similarly to Equation (41). Equations (46a-b) become

$$\frac{d^2 M(x)}{dx^2} + N(x)\frac{d^2 w(x)}{dx^2} - n(x)\frac{dw(x)}{dx} - k(x)w(x) + \rho A(x)\omega^2 w(x) = 0 \tag{47a}$$

$$M(x) = -EI(x)\frac{d^2 w(x)}{dx^2} \tag{47b}$$

A uniform grid with spacing h is assumed.

The grid at the beam's ends and at positions of discontinuity is the same as represented in Figure 8a,b.

Substituting Equations (5a), (14a-b), and (43c) into Equations (47b) and (47a) yields Equation (15b) and the following equation:

$$h^2 M_{i-1} - 2h^2 M_i + h^2 M_{i+1} + \left(\frac{N_i h^2}{EI_r} + \frac{n_i h^3}{2EI_r}\right)W_{i-1} - \left(\frac{2N_i h^2}{EI_r} + \frac{k_i h^4}{EI_r} - \beta_{Ai}\frac{\rho A_r \omega^2 h^4}{EI_r}\right)W_i$$

$$+ \left(\frac{N_i h^2}{EI_r} - \frac{n_i h^3}{2EI_r}\right)W_{i+1} = 0 \tag{48a}$$

EULER–BERNOULLI BEAM THEORY USING THE FINITE DIFFERENCE METHOD

The application of Equations (43b, d) yields

$$\omega = \lambda \times \sqrt{\frac{EI_r}{\rho A_r l_r^4}} \rightarrow \frac{\rho A_r \omega^2 h^4}{EI_r} = \beta_l^4 \lambda^2 \tag{48b}$$

For the special case of a tapered beam without an axial force or a Winkler foundation, Equation (48a) becomes

$$h^2 M_{i-1} - 2h^2 M_i + h^2 M_{i+1} + \beta_{Ai}\beta_l^4 \lambda^2 W_i = 0 \tag{48c}$$

Equations (15b) and (48a) are applied at any point on the grid. The slope and the transverse force are determined using Equations (15d) and (38), respectively.

Effect of a concentrated mass, a spring, or a spring–mass system

The analysis is conducted similarly to the section above; the transverse forces T_{il} and T_{ir} in Equations (45a-c) are calculated using Equation (38).

2.3.2 Direct time integration method

The direct time integration method developed here describes the dynamic response of the beam as multi-degree-of-freedom system. The viscosity η and an external loading p(x,t) are considered.

Uniform beam :   The governing equation is applied at any point on the beam as follows:

$$EI\frac{\partial^4 w^*(x,t)}{\partial x^4} - N(x)\frac{\partial^2 w^*(x,t)}{\partial x^2} + n(x)\frac{\partial w^*(x,t)}{\partial x} + k(x)w^*(x,t) =$$

$$p(x,t) - \rho A\frac{\partial^2 w^*(x,t)}{\partial t^2} - \eta\frac{\partial w^*(x,t)}{\partial t} \tag{49}$$

The derivatives with respect to x are formulated with Equations (4a), (4c), and (4d); those with respect to t (the time increment is Δt) are formulated considering a three-point stencil with Equations (50a-c),

$$\left.\frac{\partial w^*(x,t)}{\partial t}\right|_{i,t} = \frac{-w^*_{i,t-\Delta t} + w^*_{i,t+\Delta t}}{2\Delta t} \qquad \left.\frac{\partial^2 w^*(x,t)}{\partial t^2}\right|_{i,t} = \frac{w^*_{i,t-\Delta t} - 2w^*_{i,t} + w^*_{i,t+\Delta t}}{\Delta t^2} \tag{50a}$$

At the **initial time t = 0**, we apply a three-point forward difference approximation (Equation (8b))

$$\left.\frac{\partial^2 w^*}{\partial t^2}\right|_{i,0} = \frac{w^*_{i,0} - 2w^*_{i,\Delta t} + w^*_{i,2\Delta t}}{\Delta t^2} \qquad \left.\frac{\partial w^*}{\partial t}\right|_{i,0} = \frac{-3w^*_{i,0} + 4w^*_{i,\Delta t} - w^*_{i,2\Delta t}}{2\Delta t} \tag{50b}$$

At the **final time t =T**, we apply a three-point backward difference approximation (Equation (8d))

$$\left.\frac{\partial^2 w^*}{\partial t^2}\right|_{i,T} = \frac{w^*_{i,T-2\Delta t} - 2w^*_{i,T-\Delta t} + w^*_{i,T}}{\Delta t^2} \qquad \left.\frac{\partial w^*}{\partial t}\right|_{i,T} = \frac{w^*_{i,T-2\Delta t} - 4w^*_{i,T-\Delta t} + 3w^*_{i,T}}{2\Delta t} \tag{50c}$$

EULER–BERNOULLI BEAM THEORY USING THE FINITE DIFFERENCE METHOD

The governing equation (Equation (49)) can be formulated with FDM for x = i at time t. The FDM formulation of this equation is applied at any point of the beam at any time t using a seven-point stencil. Additional points are introduced to satisfy the boundary and continuity conditions. The boundary conditions are satisfied using a five-point stencil. Thus, the beam deflection $w^*(x,t)$ can be determined with the Cartesian model represented in Figure 16. The bending moments $M^*(x,t)$ and the shear force $V^*(x,t)$ are calculated using Equations (7a,b).
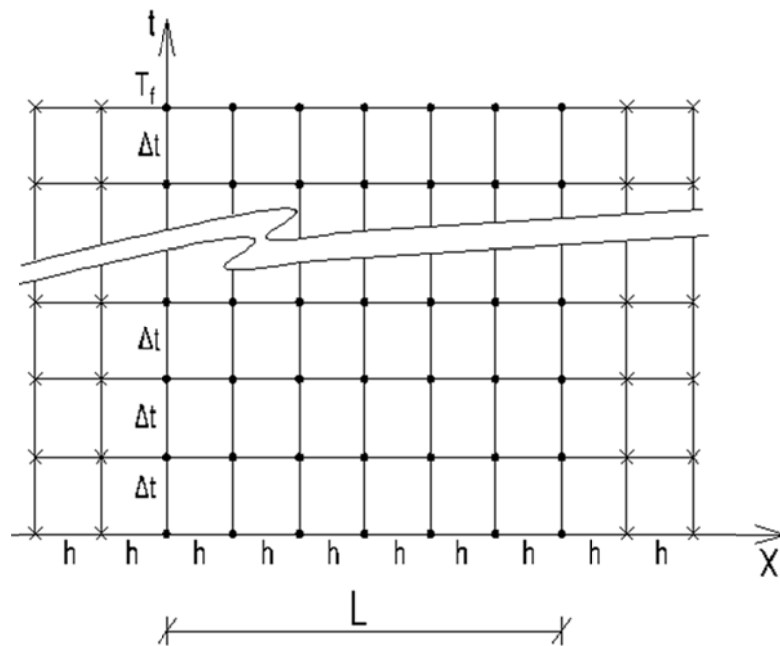
Figure 16.   Model for the calculation of time-dependent vibration of a uniform beam.

Tapered beam: a similar analysis can be conducted. Thus Equation (49) becomes

$$\frac{\partial^2 M^*(x,t)}{\partial x^2} + N(x)\frac{\partial^2 w^*(x,t)}{\partial x^2} - n(x)\frac{\partial w^*(x,t)}{\partial x} - k(x)w^*(x,t) =$$
$$-p(x,t) + \rho A(x)\frac{\partial^2 w^*(x,t)}{\partial t^2} + \eta \frac{\partial w^*(x,t)}{\partial t} \tag{51}$$

The derivatives with respect to x are formulated with Equations (14a-b); those with respect to t are formulated with Equations (50a-c).

The FDM formulation of Equations (51) and (46b) are applied at any point on the beam and at any time t using a five-point stencil and a three-point stencil, respectively. Additional points are introduced to satisfy the boundary and continuity conditions. The boundary conditions are satisfied using a three-point stencil. Thus, the bending moment

$M^*(x,t)$ and beam deflection $w^*(x,t)$ can be determined with the Cartesian model represented in Figure 17. The transverse force $T^*(x,t)$ is calculated using Equation (38).
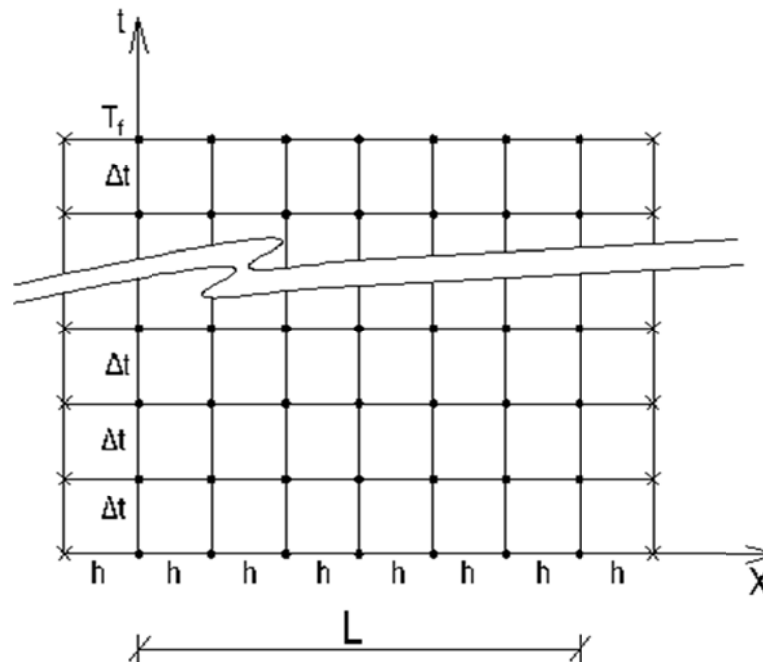
Figure 17.   Model for the calculation of time-dependent vibration of a tapered beam.

With this model, the assumptions previously made can be verified, namely the separation of variables and the harmonic vibration (Equation (41)).

2.4   Extrapolation to approximate the exact result

The analysis with the FDM is an approximation. Generally, the accuracy of the results increases by increasing the number of grid points. This means that when the number of points is infinitely high, the results tend toward the exact result. However, in first-order analysis, the exact result is rapidly obtained since the FDM polynomial approximation can match the exact results.

We assume that the relationship between the results R and the number of grid points on the beam N follows a hyperbolic curve with the constants A, B, and C, as follows:

$$R = \frac{AN + B}{N + C} \tag{52}$$

Three couples of values $(N_i \, ; \, R_i)$ are then necessary to determine A, B, and C. Solving the following equation system yields A, B, and C.

$$AN_1 + B - R_1C = R_1N_1 \tag{53a}$$

$$AN_2 + B - R_2C = R_2N_2 \tag{53b}$$

$$AN_3 + B - R_3C = R_3N_3 \tag{53c}$$

The exact result Re is approximated when the number of grid points $N \to \infty$:

$$R_e = \lim_{N \to \infty} \frac{AN + B}{N + C} = A \tag{54}$$

3   Results and discussions

3.1 First-order analysis

3.1.1 Beam subjected to a uniformly distributed load

We analyzed a uniform fixed–pinned beam subjected to a uniformly distributed load, as shown in Figure 18.
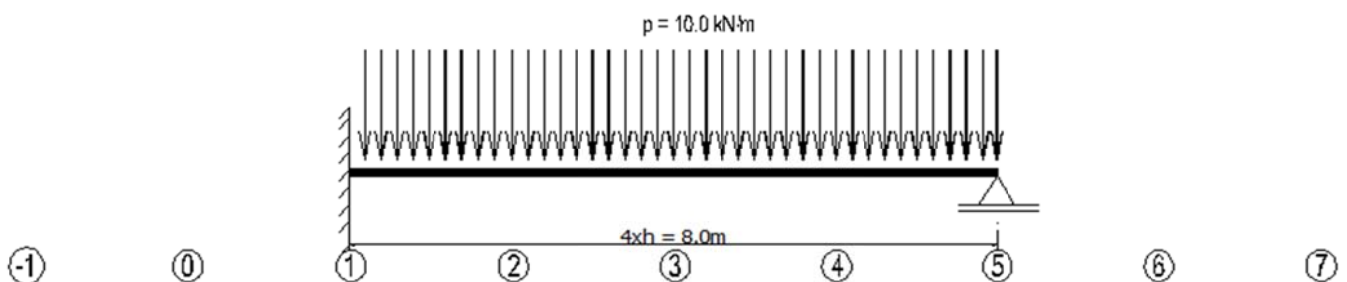
Figure 18.   Uniform fixed–pinned beam subjected to a uniformly distributed load.

The governing equation (Equation (6)) is applied at grid points 1, 2, 3, 4, and 5. The boundary conditions are satisfied using Equations (7a) and (7c).

Details of the analysis and results are presented in the supplementary material "fixed–pinned beam subjected to a uniformly distributed load". Table 1 lists the results obtained with the classical beam theory (CBT) and those obtained in the present study. Furthermore, the results are presented for a three-point stencil (TPS) considered for the slope (Equation (14b)) and bending moment (Equation (14a)) when satisfying the boundary conditions. Finally the results for a number of grid points n = 4, 3, and 2 are presented.

EULER–BERNOULLI BEAM THEORY USING THE FINITE DIFFERENCE METHOD

Table 1.   Bending moments (kNm) in the beam for various number of grid points: classical beam theory (CBT), present study, present study (three-point stencil (TPS))

	Five-point grid				Four-point grid	
	4 × 2.0m				3 × 2.67m	
Position	CBT	Present study	Present study	**Position**	CBT	Present study
X(m)	(exact results)		(TPS)	**X(m)**		
0.0	-80.00	-80.00	-72.73	0.00	-80.00	-80.00
2.0	0.00	0.00	5.45	2.67	17.78	17.78
4.0	40.00	40.00	43.64	5.33	44.44	44.44
6.0	40.00	40.00	41.82	8.00	0.00	0.00
8.0	0.00	0.00	0.00			

	Three-point grid			Two-point grid	
	2 × 4.0m			1 × 8.0m	
Position	CBT	Present study	**Position**	CBT	Present study
X(m)	(exact results)		**X(m)**		
0.00	-80.00	-80.00	0.00	-80.00	-80.00
4.00	40.00	40.00	8.00	0.00	0.00
8.00	0.00	0.00			

The results of the present study are exact for a uniformly distributed load whatever the discretization, since the exact solution for the deflection curve is here a fourth-order polynomial which corresponds to the FDM approximation. It is noted that the use of a three-point stencil for the bending moment and slope yields less accurate results since a five-point stencil is used for the governing equations.

EULER–BERNOULLI BEAM THEORY USING THE FINITE DIFFERENCE METHOD

3.1.2   Beam subjected to a concentrated load

We analyzed a uniform fixed–pinned beam subjected to a concentrated load, as shown in Figure 19.
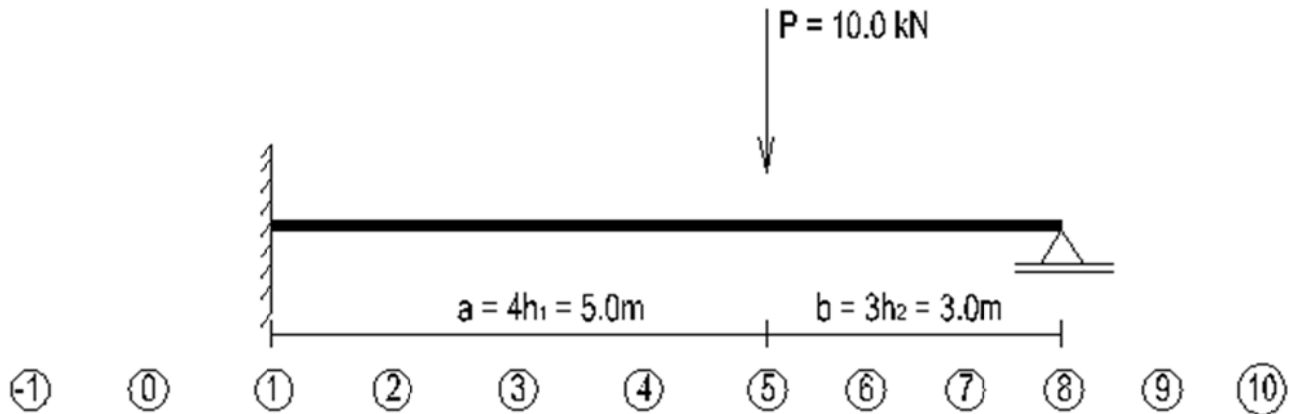
Figure 19. Uniform fixed–pinned beam subjected to a concentrated load

The model showing the grid points, as represented in Figure 5a,b, is considered.

The governing equation (Equation (6)) is applied at grid points 1, 2, 3, 4, 5l, 5r, 6, 7, and 8. The boundary and continuity conditions are satisfied using Equations (7a) and (7c), and Equations (10a-12), respectively.

Details of the analysis and results are presented in the supplementary material "fixed–pinned beam subjected to a concentrated load". Table 2 lists the results obtained with the classical beam theory (CBT) and those obtained in the present study (FDM). The results are also presented for a three-point discretization of the beam.

Table 2.   Bending moments (kNm) in the beam: CBT, FDM

Eight-point grid			Three-point grid	
4 × 1.25m + 3 × 1.0m			5.0m + 3.0m	
Position	CBT	FDM	**Position**	FDM
X(m)	(exact results)		**X(m)**	
0.00	-12.89	-12.89	0.00	-12.89
1.25	-6.19	-6.19	5.00	13.92
2.50	0.51	0.51	8.00	0.00
3.75	7.21	7.21		
5.00	13.92	13.92		
6.00	9.28	9.28		
7.00	4.64	4.64		
8.00	0.00	0.00		

EULER–BERNOULLI BEAM THEORY USING THE FINITE DIFFERENCE METHOD

The results of the present study are exact for a concentrated load whatever the discretization, since the exact solution for the deflection curve is here a third-order polynomial which is exactly described with the fourth-order polynomial FDM approximation.

3.1.3   Beam subjected to a linearly distributed load

We analyzed here a uniform fixed–pinned beam subjected to a linearly distributed load, as shown in Figure 20.
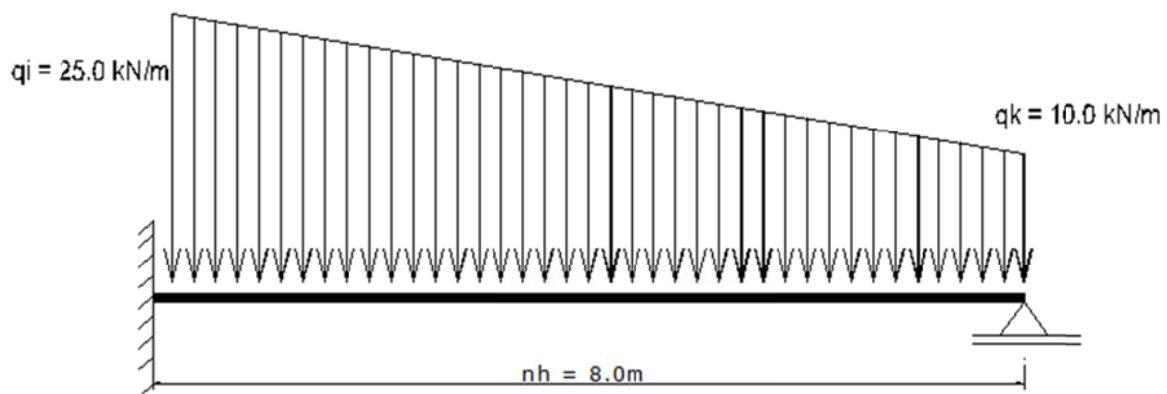
Figure 20.   Uniform fixed–pinned beam subjected to a linearly distributed load

The beam is calculated at one hand with a five-point grid, and at another hand with a six-point grid.

Details of the analysis and results are presented in the supplementary material "fixed–pinned beam subjected to a linearly distributed load". Table 3 lists the results obtained with the classical beam theory (the exact results) and those obtained in the present study (FDM).

Table 3.   Bending moments (kNm) in the beam: CBT, FDM

Position	CBT	FDM	Difference	**Position**	CBT	FDM	Difference
X(m)	(exact results)	Five-point grid	%	**X(m)**	(exact results)	Six-point grid	%
0.00	-144.00	-144.38	0.26	0.00	-144.00	-144.15	0.10
2.00	4.50	4.22	-6.22	1.60	-17.92	-18.04	0.67
4.00	68.00	67.81	-0.28	3.20	51.84	51.75	-0.17
6.00	61.50	61.41	-0.15	4.80	72.96	72.90	-0.08
8.00	0.00	0.00		6.40	53.12	53.09	-0.06
				8.00	0.00	0.00	

The results of the present study have a high accuracy. It is noted that the exact results cannot be achieved since the exact solution of w(x) for a linearly distributed loading is a fifth-order polynomial and the FDM approximation is a fourth-order polynomial. However the accuracy increases with increasing number of grid points.

EULER–BERNOULLI BEAM THEORY USING THE FINITE DIFFERENCE METHOD

3.1.4 Tapered pinned–fixed beam subjected to a uniformly distributed load

We analyzed a tapered pinned–fixed beam subjected to a uniformly distributed load, as shown in Figure 21.
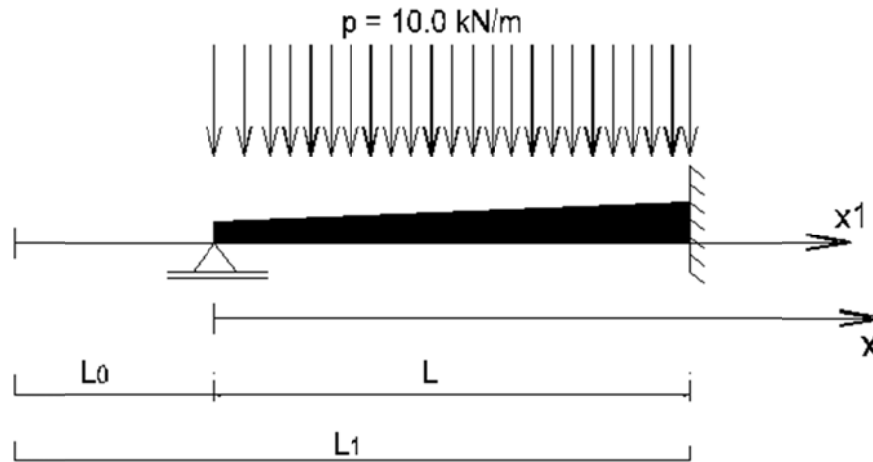
Figure 21.   Tapered pinned–fixed beam subjected to a uniformly distributed load.

At a position x_1 of the beam the second moment of area $I(x1)$ is defined as follows,

$$I(x_1) = I_1 \left(x_1 / L_1 \right)^4 ,\qquad (55)$$

I_1 is the second moment of area at $x_1 = L_1$.

   $L = 8.0m$ and $L_0 = 2.0m$

First, the beam is calculated with the force method of the classical beam theory (exact results). Then, the calculation is conducted with the FDM using n = 9, 13, and 17 grid points. The results are extrapolated to obtain those for infinite grid points. Details of the analysis and results are presented in Appendix A and in the supplementary material "tapered pinned –fixed beam subjected to a uniformly distributed load". Table 4 lists the results obtained with the classical beam theory (the exact results) and those obtained in the present study (FDM).

Table 4.   Bending moments (kNm) in the tapered beam: CBT, FDM

Position	CBT	FDM	FDM	FDM	FDM
X(m)	(exact results)	Nine-point grid	Thirteen-point grid	Seventeen-point grid	n= ∞
0.00	0.00	0.00	0.00	0.00	
2.00	17.36	17.70	17.45	17.39	17.30
4.00	-5.29	-4.61	-5.11	-5.22	-5.40
6.00	-67.93	-66.91	-67.66	-67.83	-68.10
8.00	-170.58	-169.22	-170.22	-170.44	-170.80

The results of the present study have a high accuracy.

EULER–BERNOULLI BEAM THEORY USING THE FINITE DIFFERENCE METHOD

3.2 Second-order analysis

3.2.1 Beam subjected to a uniformly distributed load and a compressive force

We analyzed a uniform fixed–free beam subjected to a uniformly distributed load and a compressive force, as shown in Figure 22.
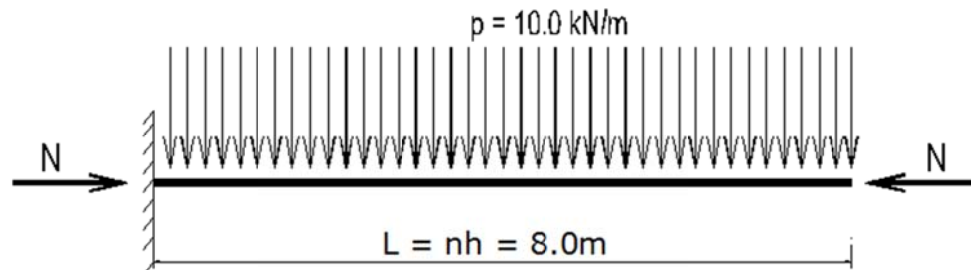
Figure 22.   Fixed–free beam subjected to a uniformly distributed load and a compressive force.

$$\frac{Nl^2}{EI} = -1.50$$

The governing equation (Equation (6)) is applied at grid points.

Details of the analysis and results are presented in the supplementary material "fixed–free beam subjected to a uniformly distributed load and compressive force". The analysis is conducted with n = 9, 13, and 17 grid points. The results are then extrapolated to obtain those for infinite grid points (Equation (54)). Table 5 lists the results obtained with the classical beam theory (CBT) and those obtained in the present study (FDM).

Table 5.   Bending moments (kNm) in the fixed–free beam: CBT, FDM

Position	CBT	FDM	FDM	FDM	FDM
X(m)	(exact results)	Nine-point grid	Thirteen-point grid	Seventeen-point grid	n= ∞
0.00	-618.05	-625.45	-621.31	-619.88	-616.93
2.00	-451.63	-457.83	-454.36	-453.16	-450.70
4.00	-282.90	-287.31	-284.84	-283.99	-282.23
6.00	-127.54	-129.79	-128.53	-128.09	-127.20
8.00	0.00	0.00	0.00	0.00	0.00

The results of the present study have a high accuracy. The extrapolation towards the exact results (n= ∞) delivers good results.

3.2.2 Buckling load of a fixed–pinned beam

We determined the buckling load of a fixed–pinned beam, as shown in Figure 23.
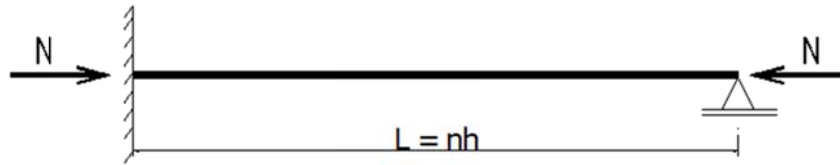
Figure 23.   Buckling load of a fixed–pinned beam.

The analysis is conducted with n = 9, 13, and 17 grid points. The results are then extrapolated to obtain those for infinite grid points. Details of the analysis and the results are listed in the supplementary material "stability of a fixed–pinned beam". The buckling load N_{cr} is defined as follows:

$$N_{cr} = -\pi^2 EI / (\beta l)^2 \tag{56}$$

Values of the buckling factor β are listed in Table 6.

Table 6.   Buckling factors of the beam: CBT, present study

CBT	FDM	FDM	FDM	FDM
(exact results)	Nine-point grid	Thirteen-point grid	Seventeen-point grid	n= ∞
0.699	0.7176	0.7073	0.7038	0.6963

The results of the present study have a high accuracy.

3.2.3 Buckling load of a tapered beam

We determined here the buckling loads of tapered beams with various support conditions, as shown in Figure 21. The analysis is conducted with n = 9, 13, and 17 grid points. The results are then extrapolated to obtain those for infinite grid points. Details of the analysis and the results are listed in the supplementary material "stability of a tapered beam". The buckling load N_{cr} is defined as follows:

$$N_{cr} = -\pi^2 EI_1 / (\beta l)^2 \tag{57}$$

The buckling factors β are listed in Table 7 for $\xi_0 = L_0/L_1 = 0.25$

Table 7.   Buckling factors β of tapered beams with $\xi_0 = L_0/L_1 = 0.25$

	FDM Nine-point grid	FDM Thirteen-point grid	FDM Seventeen-point grid	FDM $n= \infty$
Pinned–pinned	4.0255	4.0249	4.0167	4.0263
Pinned–fixed	2.8403	2.8411	2.8268	2.8396
Free–fixed	5.1245	5.1284	5.1310	5.1452
Fixed–fixed	2.4584	2.2153	2.1017	1.7884

3.3.1   Free vibration analysis of a fixed–fixed beam

We determined here the vibration frequencies of a fixed–fixed beam.

The analysis is conducted with n = 9, 13, and 17 grid points. The results are then extrapolated to obtain those for infinite grid points. The details of the analysis and results are listed in the supplementary file "vibration analysis of a fixed–fixed beam".

The coefficients λ (Equation (43c)) are listed in Table 8 below.

Table 8.   Coefficients λ of natural frequencies (first mode) of a fixed–fixed beam

CBT (exact results)	FDM Nine-point grid	FDM Thirteen-point grid	FDM Seventeen-point grid	FDM $n= \infty$
22.40	22.00	22.21	22.28	22.43

The results of the present study have a high accuracy.

3.3.2   Free vibration analysis of a tapered free–fixed beam

We determined the vibration frequencies of the tapered beam represented in Figure 24.
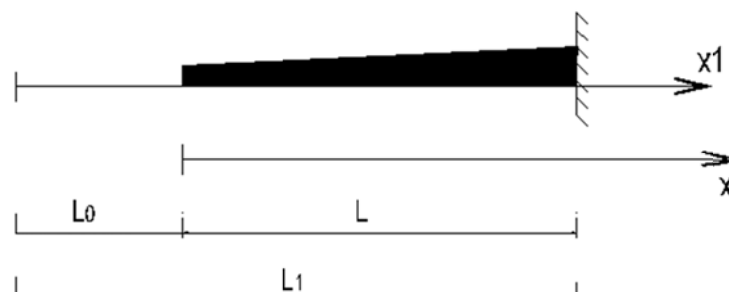
Figure 24.   Vibration analysis of a tapered free–fixed beam.

At a position x_1 of the beam, the second moment of area $I(x_1)$ is defined in Equation (55). The cross-sectional area $A(x_1)$ is defined as follows:

$$A(x_1) = A_1 \left(x_1 / L_1 \right)^2 \,,$$

(58)

A_1 being the cross-sectional area at $x_1 = L_1$. The analysis is conducted with $n = 9$, 13, and 17 grid points. The results are then extrapolated to obtain those for infinite grid points. The details of the analysis and results are listed in the supplementary file "vibration analysis of a tapered free–fixed beam".

The vibration frequency ω is defined as follows (definition adopted from Torabi [3]).

.

$$\omega = \lambda^2 \times \sqrt{\frac{EI_1}{\rho A_1 l^4}} \qquad .$$

(59)

Table 9 lists the results obtained by Torabi [3] and those obtained in the present study.

Table 9.   Coefficients λ of natural frequencies (first mode) of a tapered beam

	Torabi [3]	FDM	FDM	FDM	Present study
		Nine-point grid	Thirteen-point grid	Seventeen-point grid	$n = \infty$
$\xi_0 = 0.10$	2.6842	2.7100	2.6957	2.6906	2.6798
$\xi_0 = 0.30$	2.3471	2.3548	2.3506	2.3491	2.3459
$\xi_0 = 0.50$	2.1504	2.1493	2.1500	2.1503	2.1511
$\xi_0 = 0.70$	2.0165	2.0101	2.0137	2.0135	2.0133
$\xi_0 = 0.90$	1.9166	1.9062	1.9120	1.9157	1.9324

The results of the present study are identical to those presented by Torabi [3].

4   Conclusions

The FDM-based model developed in this paper enables, with relative easiness, first-order analysis, second-order analysis, and vibration analysis of Euler–Bernoulli beams. The results showed that the calculations conducted as described in this paper yielded accurate results. First- and second-order element stiffness matrices (the axial force being tensile or compressive) in local coordinates were determined. The analysis of tapered beams was also conducted.

The following aspects were not addressed in this study but could be analyzed with the model in future research:

✓   Analysis of Timoshenko beams.

✓   Analysis of linear structures, such as frames, through the transformation of element stiffness matrices from local coordinates in the global coordinates.

EULER–BERNOULLI BEAM THEORY USING THE FINITE DIFFERENCE METHOD

- ✓ Second-order analysis of frames free to sidesway, the P-Δ effect being examined.

- ✓ Euler–Bernoulli beams resting on Pasternak foundations.

- ✓ Elastically connected multiple-beam system.

- ✓ Warping torsion of beams.

- ✓ Lateral torsional buckling of beams.

- ✓ Classical plate theory by considering additional points at boundaries.

- ✓ Boundary value problem.

- ✓ Initial value problem.

- ✓ Linear ordinary differential equation with constants or variable coefficients.

Supplementary Materials: The following files are uploaded during submission:

- "fixed–pinned beam subjected to a uniformly distributed load"

- "fixed–pinned beam subjected to a concentrated load"

- "fixed–pinned beam subjected to a linearly distributed load"

- "tapered pinned–fixed beam subjected to a uniformly distributed load"

- "fixed–free beam subjected to a uniformly distributed load and compressive force"

- "stability of a fixed–pinned beam"

- "stability of a tapered beam"

- "vibration analysis of a fixed–fixed beam"

- "vibration analysis of a tapered free–fixed beam"

Author Contributions:

Funding:

Acknowledgments:

Conflicts of Interest: The author declares no conflict of interest.

EULER–BERNOULLI BEAM THEORY USING THE FINITE DIFFERENCE METHOD

Appendix A: Tapered pinned–fixed beam subjected to a uniformly distributed load

The tapered beam (Figure 21) subjected to a uniformly distributed load was analyzed here with the force method of the classical beam theory. The bending moment at the fixed-end was the redundant effort.

In the associated statically determinate system, $M_0(x)$ and $m(x)$ are the bending moment due to the distributed load and to the virtual unit moment at the fixed-end, respectively.

Let us introduce the dimensionless ordinate $\xi = x/l$ and $\xi_0 = L_0/L_1$.

$M_0(x)$, $m(x)$, and $I(x)$ can be expressed as follows

$$M_0(x) = px(l-x)/2 = pl^2\xi(1-\xi)/2$$
$$m(x) = x/l = \xi \tag{A1}$$
$$I(x) = I_1\left(x_1/L_1\right)^4 = I_1\left[\xi_0 + \xi(1-\xi_0)\right]^4$$

The bending moment M_1 at the fixed end is the solution of the following equations:

$$\delta_{10} = \int_0^l \frac{M_0(x) \times m(x)}{EI(x)}\,dx = \frac{pl^3}{EI_1} \times \int_0^1 \frac{\xi^2(1-\xi)}{2\left[\xi_0 + \xi(1-\xi_0)\right]^4}\,d\xi \tag{A2}$$

$$\delta_{11} = \int_0^l \frac{m(x) \times m(x)}{EI(x)}\,dx = \frac{l}{EI_1} \times \int_0^1 \frac{\xi^2}{\left[\xi_0 + \xi(1-\xi_0)\right]^4}\,d\xi \tag{A3}$$

$$M_1 = -\frac{\delta_{10}}{\delta_{11}} \tag{A4}$$

Equations (A2) and (A3) are solved numerically.

The combination of Equations (A1) and (A4) yields the bending moment at any position x, as follows:

$$M(x) = M_0(x) + M_1 \times m(x) \tag{A5}$$

Details of the results are presented in the supplementary file "tapered pinned–fixed beam subjected to a uniformly distributed load".

References

[1]   E. F. Anley, Z. Zheng. Finite Difference Method for Two-Sided Two Dimensional Space Fractional Convection-Diffusion Problem with Source Term. Mathematics 2020, 8, 1878; https://doi.org/10.3390/math8111878

[2]   M. Kindelan, M. Moscoso, P. Gonzalez-Rodriguez. Optimized Finite Difference Formulas for Accurate High Frequency Components. Mathematical Problems in Engineering. Volume 2016, Article ID 7860618, 15 pages. http://dx.doi.org/10.1155/2016/7860618

EULER−BERNOULLI BEAM THEORY USING THE FINITE DIFFERENCE METHOD

[3]   K. Torabi, H. Afshari, M. Sadeghi, H. Toghian. Exact Closed-Form Solution for Vibration Analysis of Truncated Conical and Tapered Beams Carrying Multiple Concentrated Masses. Journal of Solid Mechanics Vol. 9, No. 4 (2017) pp. 760-782

[4]   J.T. Katsikadelis. A New Direct Time Integration Method for the Equations of Motion in Structural Dynamics. Conference Paper · July 2011. Third Serbian (28th Yu) Congress on Theoretical and Applied Mechanics. https://www.researchgate.net/publication/280154205

[5]   M. Soltani, A. Sistani, B. Asgarian. Free Vibration Analysis of Beams with Variable Flexural Rigidity Resting on one or two Parameter Elastic Foundations using Finite Difference Method. Conference Paper. The 2016 World Congress on The 2016 Structures Congress (Structures16)

[6]   S. Boreyri, P. Mohtat, M. J. Ketabdari, A.Moosavi. Vibration analysis of a tapered beam with exponentially varying thickness resting on Winkler foundation using the differential transform method. International Journal of Physical Research, 2 (1) (2014) 10-15. doi: 10.14419/ijpr.v2i1.2152

[7]   K. O. Mwabora, J. K. Sigey, J. A. Okelo, K. Giterere. A numerical study on transverse vibration of Euler−Bernoulli beam. IJESIT, Volume 8, Issue 3, May 2019